JOURNAL OF VIROLOGY, Mar. 1997, p. 2202–2210 Vol. 71, No. 3
0022-538X/97/$04.00+0

Disassociation between the In Vitro and In Vivo Effects of Nitric Oxide on a Neurotropic Murine Coronavirus†

THOMAS E. LANE, ALYSSA D. PAOLETTI, AND MICHAEL J. BUCHMEIER*
Department of Neuropharmacology, The Scripps Research Institute, La Jolla, California 92037

Received 29 July 1996/Accepted 3 December 1996

Intranasal inoculation of the neuroattenuated OBLV60 strain of mouse hepatitis virus results in infection of mitral neurons in the olfactory bulb, followed by spread along olfactory and limbic pathways to the brain. Immunocompetent BALB/c mice were able to clear virus by 11 days postinfection (p.i.). Gamma interferon (IFN-γ) may play a role in clearance of OBLV60 from infected immunocompetent BALB/c mice through a nonlytic mechanism. Among the variety of immunomodulatory activities of IFN-γ is the induction of expression of inducible nitric oxide synthase (iNOS), an enzyme responsible for the production of nitric oxide (NO). Studies were undertaken to investigate the role of IFN-γ and NO in host defense and clearance of OBLV60 from the central nervous system (CNS). Exposure of OBLV60-infected OBL21a cells, a mouse neuronal cell line, to the NO-generating compound *S*-nitroso-L-acetyl penicillamine resulted in a significant decrease in viral replication, indicating that NO interfered with viral replication. Furthermore, infection of IFN-γ knockout (GKO) mice and athymic nude mice with OBLV60 resulted in low-level expression of iNOS mRNA and protein in the brains compared to that of OBLV60-infected BALB/c mice. Nude mice were unable to clear virus and eventually died between days 11 and 14 p.i. (B. D. Pearce, M. V. Hobbs, T. S. McGraw, and M. J. Buchmeier, J. Virol. 68:5483–5495, 1994); however, GKO mice survived infection and cleared virus by day 18 p.i. These data suggest that IFN-γ production in the olfactory bulb contributed to but may not be essential for clearance of OBLV60 from the brain. In addition, treatment of OBLV60-infected BALB/c mice with aminoguanidine, a selective inhibitor of iNOS activity, did not result in any increase in mortality, and the mice cleared the virus by 11 days p.i. These data suggest that although NO was able to block replication of virus in vitro, expression of iNOS with NO release in vivo did not appear to be the determinant factor in clearance of OBLV60 from CNS neurons.

The traditional view of the central nervous system (CNS) as an immunologically privileged site must be reconsidered in light of recent observations that inflammatory responses occur within the CNS in a variety of infectious and autoimmune diseases. Specific viral infections of the CNS have been shown to be effectively controlled by either humoral or cell-mediated mechanisms (6, 24, 35), and while both $CD4^+$ and $CD8^+$ T cells have been shown to be important in clearance of virus from the CNS (36, 45, 48), the exact mechanism(s) by which these cells exert their antiviral effects is enigmatic. Lysis of virally infected cells via interaction of antigen-specific, major histocompatibility complex class I-restricted $CD8^+$ cytotoxic T lymphocytes in the peripheral, non-CNS compartment is well documented (50). However, if this mechanism were to operate in the CNS, it might be disadvantageous to the host, since neurons are terminally differentiated, nondividing cells. Clearly, a relevant animal model in which neurons are preferentially infected without progression to fatal encephalitis is valuable in order to provide a more detailed understanding of the complex mechanisms by which viruses are cleared from infected neurons.

Such a model for viral clearance from CNS neurons has recently been described (36). Intranasal (i.n.) infection of mice with a neuroattenuated strain of the mouse hepatitis virus (MHV), termed OBLV60, leads to infection of neurons of the glomerular and mitral layers of the anterior olfactory bulb (36). Immunocompetent BALB/c mice clear OBLV60 between 6 and 11 days after infection. In contrast, athymic nude mice and mice depleted of both $CD4^+$ and $CD8^+$ T-cell subsets died by 11 days after infection, suggesting a requirement for T cells in viral clearance. Infection of mice selectively depleted of $CD4^+$ T cells resulted in a persistent viral infection, whereas surviving mice depleted of $CD8^+$ T cells were able to clear the infection, albeit over a longer period. These data indicated that the $CD4^+$ T-cell subset may play a more important role in CNS clearance than $CD8^+$ T cells (36).

Chemokines and cytokines can act as potent effector molecules in resolution of viral infection. Recent reports have shown that the chemokines RANTES, macrophage inflammatory proteins 1 alpha and beta, and the cytokine interleukin 16 (IL-16) produced by $CD8^+$ T lymphocytes can suppress human immunodeficiency virus replication in a noncytolytic manner (2, 8). Additional cytokines which are thought to have potent antiviral activities include gamma interferon (IFN-γ), IFN-α, IFN-β, tumor necrosis factor alpha (TNF-α), IL-2, and transforming growth factor beta (37). Feduchi et al. (14) have shown that IFN-γ and TNF-α act synergistically to block herpes simplex virus type 1 replication in HeLa or HEp2 cells. In addition, Ramsay et al. (37) demonstrated that IL-2, IFN-γ, and TNF-α are important in clearance of vaccinia virus (VV) from infected mice. Increased levels of mRNA for the cytokines IL-1α, IL-1β, IL-6, TNF-α, and IFN-γ were all observed in the brains of OBLV60-infected BALB/c mice beginning at the time of clearance, i.e., day 6 postinfection (p.i.) (36). Nude mice had similar increases in transcripts for the same cytokines with the exception of IFN-γ. By day 11 p.i., elevated cytokine messages returned to baseline levels in BALB/c mice but re-

* Corresponding author. Mailing address: The Scripps Research Institute, 10666 N. Torrey Pines Rd., CVN 8, La Jolla, CA 92037. Phone: (619) 784-7056. Fax: (619) 784-7369.

† Publication 9827-NP of The Scripps Research Institute.

mained elevated in nude mice until death. Endogenous cells of the CNS, such as microglia and astrocytes, can produce cytokines, including IL-1α, IL-1β, IL-6, and TNF-α, but not IFN-γ. These data suggested a role for IFN-γ and/or IFN-γ-producing T cells in clearance of OBLV60 from the CNS of infected mice (36).

Nitric oxide (NO) is a short-lived, gaseous, lipophilic radical that is important in transmitting cellular signals involved in vasorelaxation (32), neurotransmission (5), and mediation of host defense (33). NO is generated by the cleavage of a guanidino nitrogen atom from L-arginine by the enzyme nitric oxide synthase (NOS) (28, 34). Three isoforms of NOS have been characterized. Neuronal constitutive NOS (ncNOS; NOS-1) and endothelial constitutive NOS (ecNOS; NOS-3) both bind calmodulin, constitutively produce low levels of NO, and are regulated by calcium (34). However, in macrophages and microglia, the inducible NOS (iNOS; NOS-2) can be activated by cytokines, e.g., IFN-γ, TNF-α, IL-1, and lipolysaccharide (LPS), to produce high levels of NO over an extended period (17, 21, 27, 33, 34). With regard to host defense, iNOS activity has been shown to be a key mechanism against bacterial, fungal, and parasitic infection (33). Numerous studies have shown that NO exerts an in vitro antiviral effect on a variety of different DNA and RNA viruses, including herpes simplex virus type 1 (10, 21), VV (17, 21, 29), ectromelia virus (EV) (21), vesicular stomatitis virus (3, 4), and Friend leukemia virus (FLV) (1). The in vivo antiviral role of NO has also been examined. Production of NO has been shown to contribute to host defense against FLV (1) and EV (21) as well as coxsackievirus (26). Interestingly, an in vitro antiviral role for NO against VV has been demonstrated, yet Rolph et al. (39) have recently shown that NO may not be essential for clearance of VV in vivo. Production of NO within the CNS in response to viral infection has been shown to be either neurotoxic or neuroprotective. Various studies have demonstrated that viral infection of the CNS results in NO production which correlates with the severity of neuropathology (7, 19, 22, 49). Kreil and Eibl have reported that NO has no effect on tick-borne encephalitis virus replication in vitro and may even contribute to the pathogenesis of disease in vivo (23). NO is thought to contribute to CNS damage and demyelination in rodents suffering from experimental allergic encephalitis and has been shown to be toxic to cultured oligodendrocytes (25, 30). Conversely, NO has also been suggested to be an important component of host defense against CNS viral infections by either interfering with viral replication (3, 4) or enhancing the ability of infected cells to cope with viral infection (47). It is of interest to consider whether NO can function in clearance of OBLV60 from neurons in infected mice. NO is an attractive candidate for a CNS effector molecule because it readily diffuses across the cell membrane; thus, its actions are independent of immune recognition (21, 33). The purpose of these studies was to determine the roles of IFN-γ and NO in host defense following OBLV60 infection of the CNS.

MATERIALS AND METHODS

Cell culture. OBL21a is a mouse neuronal cell line developed by integration of a retroviral vector encoding the avian *myc* oncogene into primary tissue from the olfactory bulb of newborn CD-1 mice (40). The DBT cell line is a mouse astrocytoma routinely used for determining titers of MHV (18). Both OBL21a and DBT cells were maintained in Dulbecco modified Eagle medium containing 10% heat-inactivated fetal bovine serum (Hyclone Laboratories) and supplemented with 15 mM HEPES, 100 U of penicillin per ml, and 100 mg of streptomycin per ml.

Reagents. *S*-Nitroso-L-acetyl penicillamine (SNAP), which releases NO in aqueous solutions with a half-life of approximately 4 h (20), was purchased from Calbiochem, San Diego, Calif. *N*-Acetyl-penicillamine (NAP), which is the nonnitrosylated form of SNAP and does not release NO in solution, LPS (*Escherichia coli* serotype O111:B4), and aminoguanidine (AG) hemisulfate salt were purchased from Sigma Immunochemicals, St. Louis, Mo. A 1.8-kb cDNA probe for mouse iNOS mRNA was purchased from Alexis Biochemicals, San Diego, Calif.

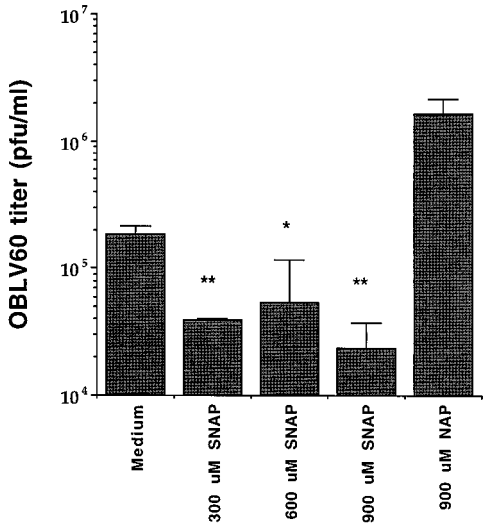

FIG. 1. Treatment of OBLV60-infected OBL21a cells with SNAP inhibits viral replication. The antiviral effect of NO-generating SNAP was compared with that of its control, NAP. OBLV60-infected OBL21a cells were exposed to the indicated concentrations of SNAP or NAP. Fresh SNAP and NAP were added every 6 h for 24 h. The results are means ± standard deviations for a total of three experiments. *, $P \leq 0.02$; **, $P \leq 0.001$.

Antiviral assays. For studies designed to assess the in vitro antiviral activities of NO on OBLV60 replication, six-well, flat-bottom plates (Becton Dickson Laboratories) were seeded with OBL21a cells, which were infected with OBLV60 at a multiplicity of infection of 0.1. Control monolayers received medium only. Virus was allowed to adsorb for 1 h, at which time the monolayers were washed with prewarmed (37°C) Hanks' balanced salt solution, and the monolayers were then incubated in 3 ml of medium supplemented with 2.5 mM L-cysteine alone (21) or containing 300, 600, or 900 μM SNAP or 900 μM NAP. Fresh SNAP was added every 6 h for a 24-h incubation period, after which supernatants were collected and viral titers were determined by plaque assays with DBT cells as described by Gallagher et al. (16).

Virus and mice. OBLV60 is a previously described 60-day isolate obtained during passage of the neurovirulent MHV type 4 in the mouse neuronal cell line OBL21a (16). Seven- to 13-week-old BALB/c ByJ mice, athymic nude mice, and IFN-γ knockout mice (GKO mice, animals with a targeted disruption of the IFN-γ gene) (12) were inoculated i.n. with 1,000 PFU of OBLV60 in a total volume of 10 μl and sacrificed by methoxyflurane anesthesia at days 3, 5, 6, 7, 11, 14, 18, and 32 p.i. (depending on the experiment). All animals used were of the *H-2*^{d} background. Sham-infected animals received 10 μl of medium only. One half of the brain from each animal was used for plaque assay to determine viral titer, and the remaining half was used for either total RNA extraction, immunohistochemistry, or in situ hybridization.

AG treatment of mice. AG is a selective inhibitor of iNOS activity which readily crosses the blood brain barrier (9, 11, 31). In experiments designed to assess the in vivo effects of AG treatment on OBLV60-infected BALB/c mice, animals were divided into four groups: OBLV60-infected animals receiving AG or phosphate-buffered saline (PBS) and sham-infected animals receiving AG or PBS. Mice were injected intraperitoneally (i.p.) with either 4 mg of AG (dissolved in 0.5 ml of PBS) or 0.5 ml of PBS alone. Animals were injected again with either 4 mg of AG or PBS and then inoculated i.n. with 1,000 PFU of OBLV60 or medium alone. The experiment followed an 11-day time course, with mice being injected twice daily with either AG (for a total of 8 mg/day) or PBS. The animals were sacrificed as described above on days 3, 7, and 11 p.i., and one half of the brain was used for determining viral titers and the remaining half was used for either RNA extraction, histology, or immunohistochemistry. In order to determine if AG at the dosage used was able to effectively block in vivo iNOS activity, mice were injected i.p. with 4 mg of AG (dissolved in 0.5 ml of PBS) or 0.5 ml of PBS for 6 h before and after i.p. injection of 10 μg of LPS. Blood samples were collected at 0 and 18 h, and plasma samples were obtained by spinning blood through an Ultrafree-MC column (Millipore Corp., Bedford, Mass.) at 14,000 × *g* for 30 min at 4°C. Levels of NO_2^- and NO_3^- (NO_2^-/NO_3^-) (stable degradation products of NO) in plasma were determined by using the protocol from the Cayman nitrite/nitrate assay kit (Alexis Biochemicals).

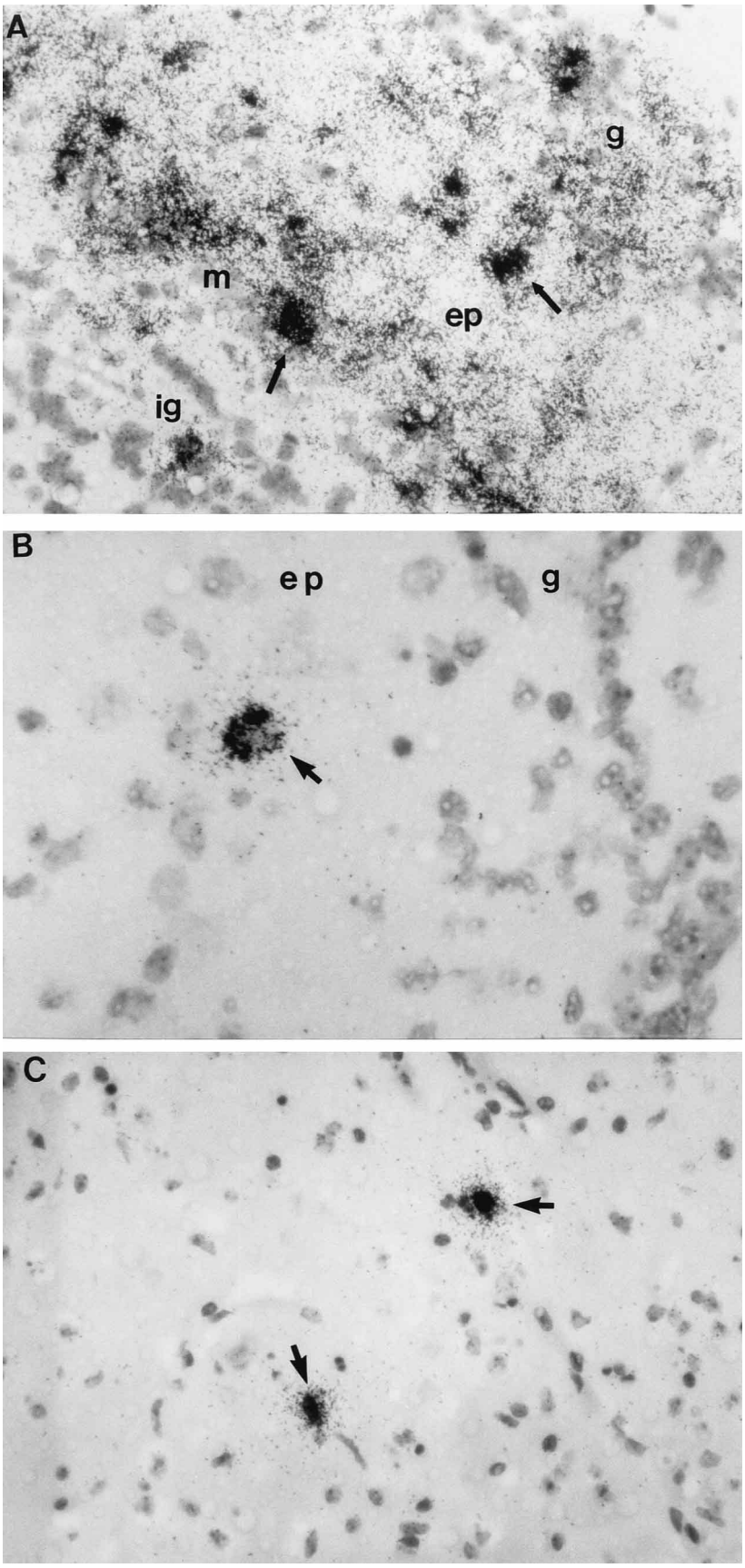
A
g
m
ep
ig
B
ep
g
C

Reverse transcription-PCR (RT-PCR). Following i.n. inoculation, brains and spleens were collected at various times p.i. and total RNA was isolated by using TRIzol reagent (GibcoBRL, Gaithersburg, Md.). cDNA was generated by using 1 μg of total RNA from each tissue according to a previously established protocol (41). Primers for PCR amplification of the mouse macrophage iNOS and control glyceraldehyde-3-phosphate dehydrogenase (G3PDH) were purchased from Clonetech Laboratories, Inc., San Francisco, Calif. PCR amplification for both molecules was performed with a Perkin-Elmer model 480 DNA thermal cycler with the following profile: step 1, initial denaturation at 94°C for 45 s; step 2, annealing at 65°C (iNOS) or 60°C (G3PDH) for 45 s; and step 3, extension at 72°C for 2 min. Steps 1 to 3 were repeated 34 times for a total of 35 cycles for each molecule. A final extension at 72°C for 7 min was performed. The amplified products were analyzed on a 1.8% agarose gel containing 0.5 μg of ethidium bromide per ml and extracted by using the Gene Clean II system (Bio 101, San Diego, Calif.) and cloned into the pCR Script SK (+) vector (Stratagene, San Diego, Calif.). Double-stranded plasmid clones were sequenced by the primer-directed dideoxy chain termination method with dye-labeled terminators, using a Prism Terminator kit (Applied Biosystems Inc., Foster City, Calif.) with a model 373A DNA sequencer (Applied Biosystems). To distinguish PCR errors, the sequences of four individual clones were examined. iNOS nucleotide sequences were analyzed by using the MacVector sequence analysis program, version 3.5 (Kodak, New Haven, Conn.).

Dot blot analysis. Confirmation that the PCR products detected from mice by using iNOS primers were in fact iNOS was made by Southern blotting using a 1.8-kb cDNA probe for mouse iNOS (Alexis Biochemicals). Endpoint dilution analysis was performed by using PCR products dot blotted onto Biotrans nylon membranes (ICN Pharmaceuticals Inc., Costa Mesa, Calif.) and probed with a ^{32}P-labeled cDNA iNOS probe (100 ng) (DECAprime II DNA labeling kit; Ambion, Inc., Austin, Tex.). As an internal control, G3PDH PCR products from the same animals in which iNOS mRNA was detected were subjected to endpoint dilution analysis as described for the iNOS products. A ^{32}P-labeled cDNA probe for G3PDH was used to detect the PCR products. Following overnight hybridization at 42°C, the blots were subjected to high-stringency washes, dried, and set up for autoradiography using Kodak X-Omat film. The film was exposed overnight at −70°C and developed.

In situ hybridization. In situ hybridization of brain sections for virus was performed by using a 473-bp fragment of the S gene from OBLV60. This fragment was cloned into the pCR Script SK (+) vector (Stratagene) and was flanked by T3 and T7 promoter sites. The antisense probe was generated by linearizing the construct by digestion with *Not*I and using the T7 polymerase, while the sense probe was generated by an *Eco*RI digestion and transcription using the T3 polymerase. A probe for mouse IFN-γ was kindly provided by Regula Mueller (The Scripps Research Institute). A 737-bp fragment was cloned into the Sp64 vector with a flanking SP6 promoter site. Both an antisense construct and a sense construct were made, and the SP6 polymerase was used for transcription of both probes. The ^{35}S-UTP-radiolabeled RNA probes were derived by in vitro transcription reaction with an RNA transcription kit (Stratagene). Brain tissue was fixed in 10% normal buffered formalin prior to being processed in paraffin blocks. Six-micrometer-thick sections of brain were cut and floated on Vectabond (Vector Laboratories, Burlingame, Calif.)-treated Superfrost slides (Fisher, Pittsburgh, Pa.), dried overnight, and dewaxed. The slides were submerged in 50 μg of proteinase K (Fisher) per ml in proteinase K buffer (500 mM NaCl, 10 mM Tris [pH 8.0], 5 mM EDTA) for 20 min and then washed twice in 0.5× SSC (1× SSC is 0.15 M NaCl plus 0.015 M sodium citrate). The slides were prehybridized with 100 μl of 2× SSC–50% formamide–10% dextran sulfate–1× Denhardt's solution and incubated at 46°C for 1 h. ^{35}S-labeled riboprobe (3×10^6 cpm) was added to the slides in a 50-μl volume, and hybridization was allowed to occur overnight at 46°C. The slides were washed twice in 2× SSC–1 mM EDTA and then immersed in 20 μg of RNase A per ml in RNase buffer (500 mM NaCl, 10 mM Tris [pH 8.0]) for 30 min at room temperature. The slides were then washed twice with 2× SSC–1 mM EDTA at room temperature, subjected to two 1-h incubations with 0.2× SSC–1 mM EDTA at 42°C, and washed twice with 0.5× SSC at room temperature. The slides were dehydrated and dried. Next, the slides were dipped in a Kodak NTB2 nuclear emulsion at 42°C and exposed at 4°C for 2 to 4 weeks in a desiccator. The slides were developed and fixed with Kodak D-19 developer and fixer, counterstained with hematoxylin and eosin Y solutions, dehydrated, and mounted.

Immunohistochemistry. Anti-mouse iNOS antibody (rabbit polyclonal anti-iNOS; Transduction Laboratories, Lexington, Ky.) was used to detect iNOS expression in the brains of OBLV60-infected mice. Staining for iNOS was performed on brain tissue fixed in 10% normal buffered formalin and embedded in paraffin. Following dewaxing and rehydration, the sections were treated with 0.3% hydrogen peroxide solution and then boiled in 250 ml of 0.01 M citrate buffer (pH 6.0) for 3 min and simmered for 15 min. After this treatment, the sections were allowed to stand at room temperature for 20 min in the citrate buffer, washed in PBS, and then incubated for 30 min at room temperature with PBS containing 5% normal goat serum (Vector Laboratories) and 0.1% Triton X-100. The sections were washed with PBS and then incubated with the diluted primary antibody for iNOS (1:100 dilution in 2% normal goat serum in PBS) overnight at 4°C with slight shaking. Following overnight incubation, the sections were washed with PBS and incubated for 1 h with biotinylated secondary antibody (1:300) and treated with a Vectastain ABC Elite kit (Vector Laboratories) according to manufacturer specifications. VIP peroxidase (Vector Laboratories) was used as the final substrate. Finally, the sections were counterstained with hematoxylin, dehydrated, coverslipped, and examined by light microscopy. Normal rabbit antibody immunoglobulin G was used as a control for primary antibody.

Statistical analyses. Statistical analyses were performed by the Student *t* test.

RESULTS

SNAP-generated NO inhibits OBLV60 replication. OBLV60-infected OBL21a cells were treated with SNAP and the control reagent NAP for 24 h, and viral titers from the supernatant were determined. As shown in Fig. 1, there is a significant decrease in viral titers obtained from SNAP-treated monolayers compared to those of monolayers treated with either medium alone or medium containing NAP. The NO-induced decrease in viral titers did not appear to be due to toxic effects, as SNAP-treated cells had a viability of >90% as determined by trypan blue exclusion. The SNAP-induced effect on OBLV60 replication in OBL21a cells did not appear to be strictly dose dependent over the range tested, as only slight differences in viral titers were evident in monolayers treated with 300 or 900 μM SNAP. SNAP did not have a viricidal effect on the virus, since exposure of OBLV60 to 1 mM SNAP for 24 h did not affect the ability of the virus to infect and replicate in DBT cells (data not shown). These data suggest that NO is able to effectively inhibit OBLV60 replication in transformed neurons. Increased titers on NAP-treated monolayers relative to those on control monolayers were noted. We have observed this effect on OBLV60 replication with 300, 600, and 900 μM NAP; thus, it does appear to be concentration dependent (data not shown). The effects NAP may have on either virus and/or cells which result in enhanced viral replication are unknown.

Detection of IFN-γ mRNA and viral RNA by in situ hybridization. It has been suggested that IFN-γ plays an important role in clearance of OBLV60 from infected BALB/c mice (36). We were interested in determining the spatial relationship between IFN-γ mRNA-positive cells and viral RNA. With ^{35}S-labeled riboprobes for OBLV60 and IFN-γ, in situ hybridization was performed on brain sections from OBLV60- and sham-infected mice. The results shown in Fig. 2 illustrate that areas of viral RNA expression correspond with IFN-γ mRNA expression. Viral RNA was located predominantly in the mitral layer, as was IFN-γ mRNA; however, IFN-γ message was also observed in the external plexiform layer of the olfactory bulb (Fig. 2A and B). IFN-γ message was not strictly restricted to the olfactory bulb; signal was detected in other areas of the brain, particularly along the myelinated anterior olfactory nerve tract, in which viral RNA was also detected (Fig. 2C).

FIG. 2. (A) Viral RNA in olfactory bulb 6 days p.i. OBLV60 RNA is detected by in situ hybridization in the olfactory bulb of a BALB/c mouse 6 days p.i. As previously demonstrated (36), viral RNA is found predominantly in neurons of the mitral layer, although viral RNA is also detected in the glomerular layer. Infected neurons are indicated (arrows). g, glomerular layer; ep, external plexiform layer; m, mitral layer; ig, internal granule layer. Original magnification, ×400. (B) IFN-γ mRNA in olfactory bulb of OBLV60-infected mice. In situ hybridization shows a cell (arrow) expressing IFN-γ mRNA in the external plexiform layer of the olfactory bulb 6 days following i.n. inoculation with OBLV60. g, glomerular layer; ep, external plexiform layer. Original magnification, ×600. (C) IFN-γ mRNA along anterior olfactory tract. In situ hybridization shows cells positive for IFN-γ mRNA (arrows) in the region of the olfactory nerve 6 days following i.n. inoculation with OBLV60. Original magnification, ×400.

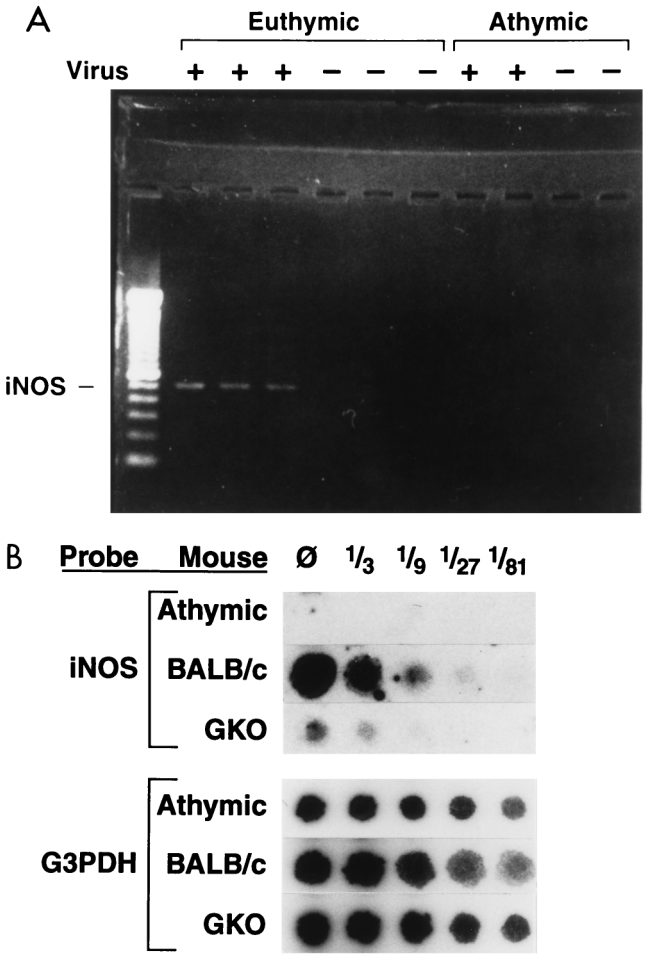

FIG. 3. (A) iNOS mRNA is expressed in brains of OBLV60-infected mice. iNOS mRNA was RT-PCR amplified from the brains of OBLV60-infected BALB/c and nude mice at day 6 p.i. and run on a 1.8% agarose gel. +, viral infection; −, sham infection. The expected-size PCR product for iNOS (approximately 500 bp) is indicated on the left. Each lane represents an individual mouse from an independent experiment. Molecular size markers are a 100-bp ladder. (B) Dilution of iNOS PCR product. iNOS PCR products from OBLV60-infected BALB/c, nude (athymic), and GKO mice were serially diluted, blotted onto nylon membranes, and probed with a ^{32}P-labeled 1.8-kb cDNA probe specific for mouse iNOS as described in Materials and Methods. As an internal control, G3PDH PCR products were included and probed with a ^{32}P-labeled probe. PCR products (both iNOS and G3PDH) from BALB/c and nude mice are from day 6 p.i., while PCR products from GKO mice are from day 7 p.i. Numbers indicate dilutions of PCR products. **Ø**, undiluted products.

Pearce et al. (36) have previously demonstrated that both $CD4^+$ and $CD8^+$ T cells were present in the olfactory bulbs of infected mice at 6 days p.i., and it is likely that these cells were responsible for IFN-γ mRNA expression. No detectable levels of viral RNA or IFN-γ mRNA were present in the brains of sham-infected animals (data not shown).

OBLV60-infected BALB/c mice produce iNOS mRNA and protein. We were interested in determining whether both iNOS mRNA and protein were expressed in the brains of OBLV60-infected animals. As shown in Fig. 3A, a PCR product consistent with iNOS mRNA was detected in the brains of OBLV60-infected BALB/c mice at day 6 p.i. In contrast, iNOS mRNA was barely detectable in infected nude mice at the same time point. An endpoint dilution analysis was performed on the PCR products from both OBLV60-infected BALB/c and nude mice in order to more closely compare concentration differences between iNOS amplicons. The results in Fig. 3B indicate that iNOS mRNA is more prevalent in infected BALB/c mice than in infected nude mice. iNOS message was not detected in brains of sham-infected BALB/c and nude mice, suggesting that expression was the result of the host inflammatory response to viral infection of the brain (data not shown).

To quantitate the increase in iNOS-expressing cells in the brains of infected mice, we counted immunohistochemically stained cells in multiple sections from BALB/c, GKO, and nude mice. These data are presented in Fig. 4 and show a marked increase in the numbers of iNOS-positive cells in BALB/c mice after infection. In both BALB/c and nude mice, low numbers of positive cells per section were detected at days 3 and 5 p.i. but the number of positive cells in BALB/c mice increased dramatically at 6 days p.i. (Fig. 4). The observed increase in iNOS expression at day 6 p.i. correlates with production of IFN-γ mRNA. The number of positive cells decreased slightly from days 6 to 7 p.i. and eventually returned to baseline levels by day 11 p.i. (Fig. 4). The majority of iNOS-positive cells present at day 6 p.i. were detected within the mitral and glomerular layers as well as the external plexiform layer of the olfactory bulb, with very limited staining found outside the olfactory bulb. iNOS-positive cells in infected BALB/c mice phenotypically resembled both microglia/macrophages and astrocytes (Fig. 5). In contrast to OBLV60-infected BALB/c mice, infected nude mice showed only a marginal increase in iNOS-positive cells at day 6 p.i. which then returned to baseline levels at day 11 p.i. (Fig. 4).

Treatment of OBLV60-infected mice with AG does not affect viral clearance. AG is a selective inhibitor of iNOS activity, and treatment of rodents with AG has been shown to effectively neutralize CNS iNOS (9, 11, 31). To determine whether iNOS expression was essential for viral clearance, OBLV60-infected mice were treated with AG in order to determine their ability to eliminate virus from the CNS. Daily administration of AG by i.p. injection had no effect on the ability of the mice to

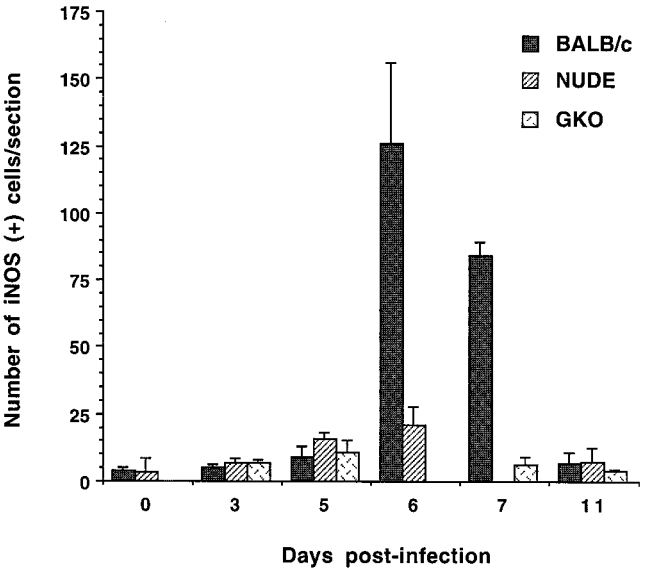

FIG. 4. Induction of iNOS in brains of OBLV60-infected mice. Brains were removed at the indicated times, and sagittal sections were stained for iNOS protein as described in Materials and Methods. The number of iNOS-positive cells in the olfactory bulb were counted from a minimum of two sections per mouse, and results are means ± standard deviations.

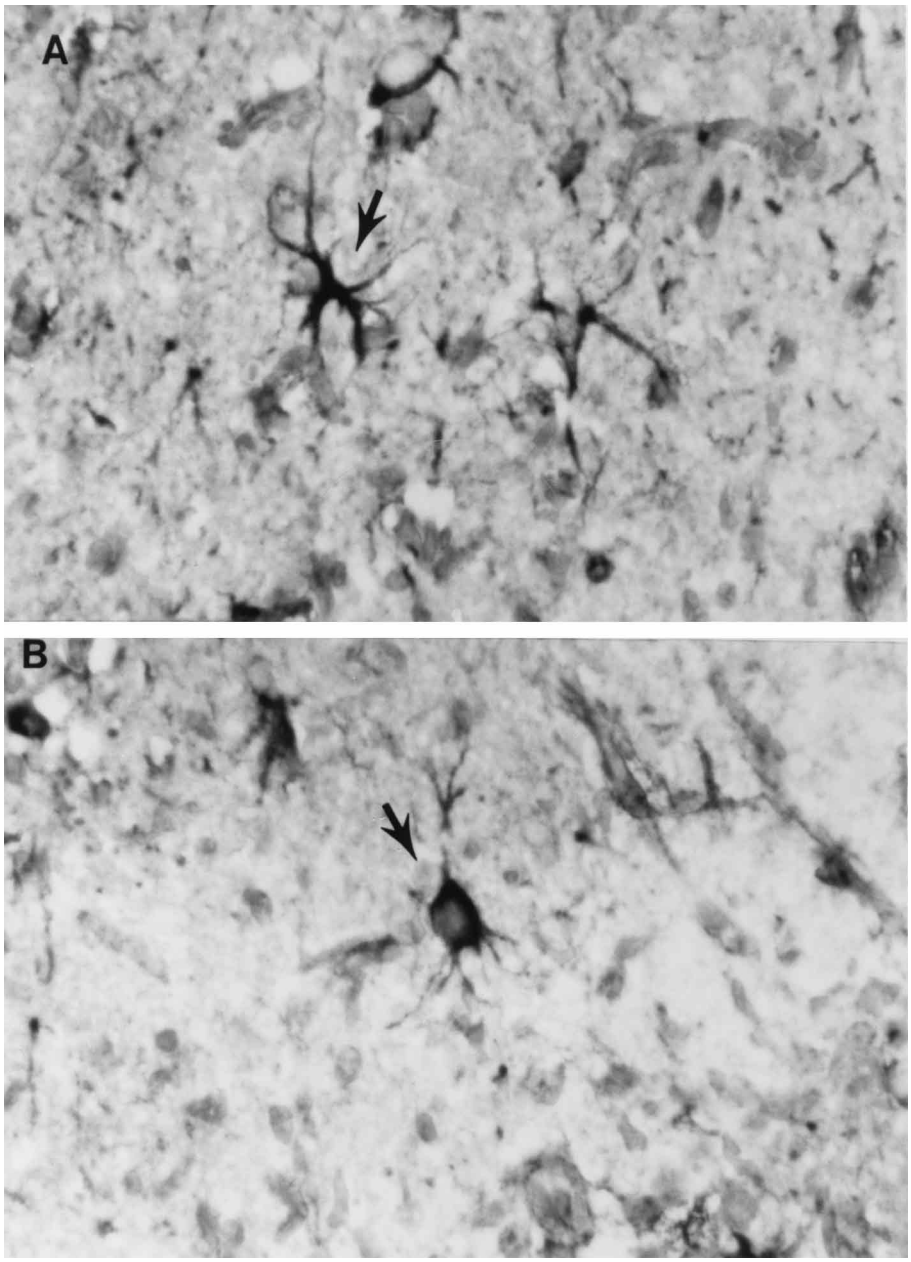

FIG. 5. iNOS-positive cells in olfactory bulb. Typical results of iNOS staining in the olfactory bulb of an OBLV60-infected BALB/c mouse 6 days p.i. are shown. iNOS-positive cells are seen in the external plexiform layer (A and B). Original magnification, ×600.

clear OBLV60 compared to that of infected mice treated with PBS alone (Fig. 6A). At day 3 p.i., AG-treated mice exhibited slightly lower titers of virus than infected control mice, but this differential was not evident 7 days after infection. The AG treatment regimen used was sufficient to block in vivo iNOS activity, as indicated by the inability of AG-treated animals to produce increased levels of NO_2^-/NO_3^- in plasma following LPS injection (Fig. 6B). We were unable to show a direct effect on NO_2^-/NO_3^- levels in plasma of OBLV60-infected BALB/c mice, as these animals do not display increased levels of NO_2^-/NO_3^- in plasma at any point following infection (data not shown). This most likely is because iNOS mRNA could be detected only in the brain and not in other organs examined. Thus, NO production in response to OBLV60 infection appears to be limited only to the CNS. Examination of brains of infected AG-treated mice revealed histopathology similar to that of infected BALB/c mice (data not shown). These data suggest that iNOS or NO does not play a primary role in clearance of OBLV60 from the CNS.

Clearance of OBLV60 in GKO mice is delayed. Mice with a targeted disruption of the IFN-γ gene were examined for their ability to clear OBLV60. These mice have previously been shown to exhibit multiple defects in immune function, including the inability to produce NO following infection with *Mycobacterium bovis* (12). Furthermore, i.p. injection of GKO mice with 10 μg of LPS did not result in a marked increase in NO_2^-/NO_3^- levels in plasma (Fig. 6B). Because of these observations, GKO mice were infected i.n. with OBLV60 in order

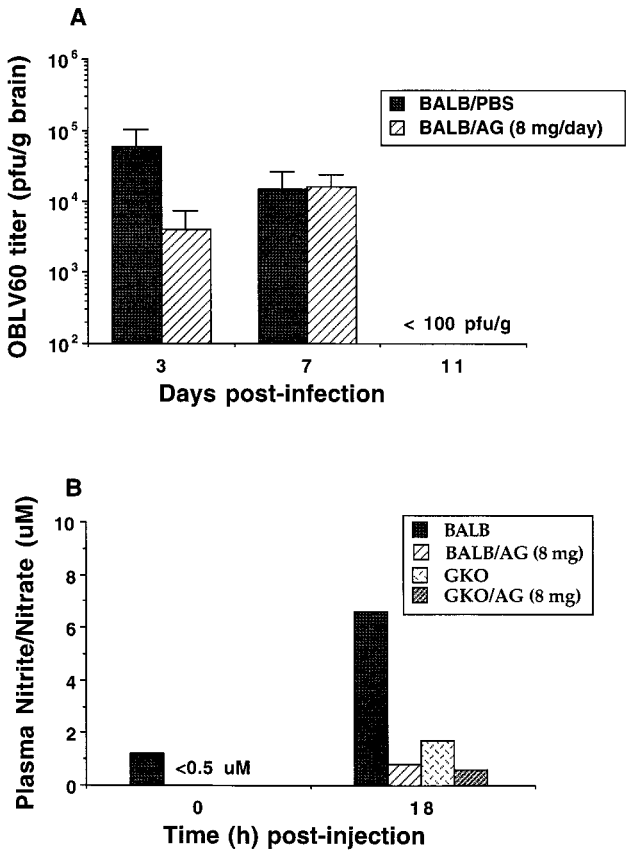

FIG. 6. (A) Clearance of OBLV60 in mice treated with AG. OBLV60-infected mice were treated daily with 8 mg of AG for a total of 11 days, and viral titers from the brain were determined at days 3, 7, and 11 p.i. Virus was cleared to below the limit of detection (100 PFU/g). Mean virus titers from groups of two mice are shown; error bars are standard deviations. (B) I.p. injection of AG blocks LPS-induced iNOS activity. BALB/c and GKO mice were injected i.p. with 4 mg of AG or PBS 6 h prior to i.p. injection with 10 μg of LPS. After 6 h, mice were again injected i.p. with either 4 mg of AG or PBS. Blood samples were collected at the indicated times and plasma NO_2^-/NO_3^- levels were determined as described in Materials and Methods. Two mice were used for each condition examined.

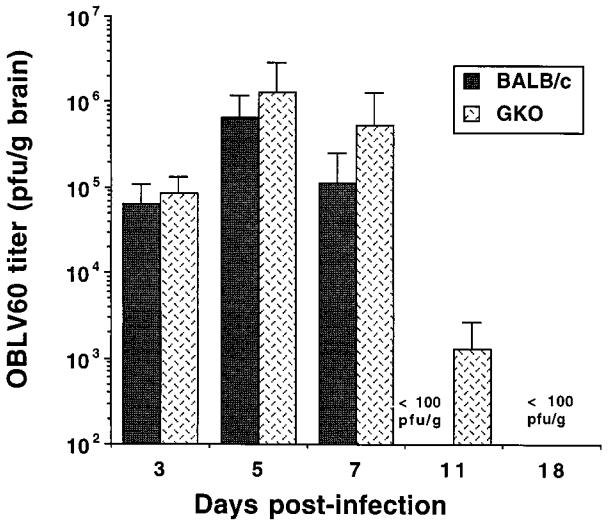

FIG. 7. Delayed clearance of OBLV60 in GKO mice. GKO and BALB/c mice were infected i.n. with 1,000 PFU of OBLV60 and viral titers from the brain were determined by plaque assay on days 3, 5, 7, and 11 p.i. Virus was cleared below the limits of detection (100 PFU/g) by 11 days after infection in normal BALB/c mice, while GKO mice cleared detectable levels of virus at day 18 p.i. Mean virus titers from groups of six mice are shown; error bars are standard deviations.

to determine whether the ability to clear virus from the CNS was compromised. As shown in Fig. 7, infected GKO mice exhibited delayed clearance of virus from the brain compared with that of infected BALB/c mice (Fig. 7); however, all GKO mice eventually cleared virus by day 18 p.i. RT-PCR analysis of RNAs obtained from brains of OBLV60-infected GKO mice revealed that iNOS mRNA was produced at days 5 and 7 p.i. and declined to baseline levels by day 11 p.i. (Fig. 8). A comparison of iNOS mRNA levels between infected BALB/c and GKO mice by endpoint dilution analysis shows that iNOS is present in higher levels in the brains of BALB/c mice (Fig. 3B). The low level of iNOS mRNA at day 7 p.i. is also reflected in the low number of iNOS-positive cells in the brain compared to that of BALB/c mice at the same time point (Fig. 4). In fact, immunohistochemical analysis revealed only a marginal increase in iNOS-positive cells in the brains of infected GKO mice during the course of infection, which returned to baseline levels by day 11 p.i. (Fig. 4).

DISCUSSION

Both BALB/c and athymic nude mice exhibited increased expression of multiple cytokine mRNAs in the CNS following infection with the neuroattenuated MHV strain OBLV60 (36). Although the profiles and kinetics of cytokine production were almost identical for the two populations of mice, IFN-γ was produced in infected BALB/c mice but was barely detectable in infected nude mice. Given that OBLV60-infected BALB/c mice survive infection while nude mice do not, these data suggested that IFN-γ may play an important role in viral clearance.

In vitro studies have demonstrated that IFN-γ alone or in combination with other stimulatory signals is able to induce an antiviral state in infected macrophages through iNOS production of NO (10, 17, 21). In vivo studies have shown that NO production is an important component of host defense against various viruses, including EV (21), FLV (1), and coxsackievirus (27). NO is also an attractive CNS antiviral effector molecule

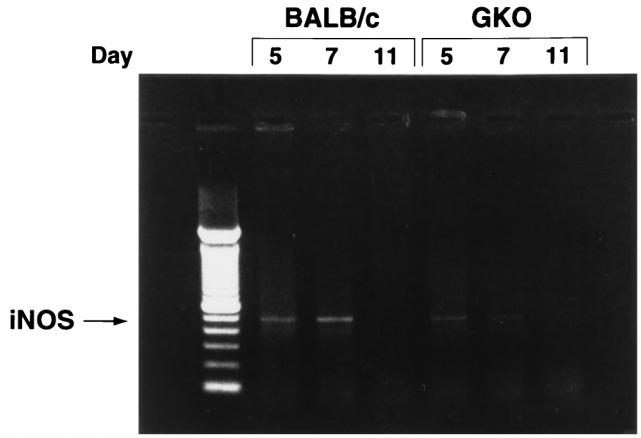

FIG. 8. iNOS mRNA is expressed in brains of OBLV60-infected GKO mice. iNOS mRNA was RT-PCR amplified from the brains of OBLV60-infected BALB/c and GKO mice at 5, 7, and 11 days p.i. The expected-size PCR product for iNOS (approximately 500 bp) is indicated on the left. Molecular size markers are a 100-bp ladder.

in that it is able to exert a nonlytic antiviral effect and to function in the absence of specific immune recognition (10, 21). These studies were undertaken to determine what roles IFN-γ and NO have in clearance of OBLV60 from the CNS of OBLV60-infected mice.

In vitro studies using the NO donor SNAP demonstrated that NO is able to block viral replication in a mouse neuronal cell line. Furthermore, NO did not exert a viricidal effect on OBLV60, suggesting that an antiviral effector mechanism may be acting at the level of the infected cell following exposure to NO. These observations are consistent with other reports demonstrating that SNAP-generated NO is able to block viral replication (1, 10, 17, 21). Harris et al. (17) have recently shown that NO blocks intracellular VV replication by inhibiting late protein synthesis, DNA replication, and viral particle formation. Whether any of these mechanisms are occurring in SNAP-treated OBL21a neuronal cells is currently unknown.

Infection of BALB/c mice with OBLV60 results in increased production of iNOS mRNA and protein in the olfactory bulb at day 6 p.i. which then returns to baseline levels at day 11 p.i., as measured by RT-PCR and immunohistochemical analysis, respectively. The iNOS-positive cells phenotypically resembled microglia/macrophages and astrocytes. Combined with the observation by Pearce et al. (36) that both activated microglia/macrophages and astrocytes are present in the olfactory bulb of infected BALB/c mice at day 6 p.i. and with reports demonstrating that activated microglia and astrocytes can express iNOS, these results are not surprising (21, 42). The presence of iNOS protein in the olfactory bulbs of infected BALB/c mice correlates with the influx of $CD4^+$ and $CD8^+$ T lymphocytes, the expression of IFN-γ mRNA, and the onset of viral clearance. These data suggest that iNOS or NO may play an important role in clearance of OBLV60 from the CNS of infected mice. Alternatively, expression of iNOS may simply reflect the fact that IFN-γ is activating various cell types to produce iNOS as well as a host of other immunomodulatory factors. In order to distinguish between these two possibilities, we treated OBLV60-infected BALB/c mice with the iNOS inhibitor AG and evaluated the kinetics of viral clearance. AG-treated mice cleared virus in the same time frame (11 days) as PBS-treated mice. The dosage of AG used for these studies (8 mg/day) was sufficient to effectively block an LPS-induced increase in NO_2^-/NO_3^- levels in plasma, presumably by blocking iNOS activity. These data imply that alternative mechanisms rather than iNOS or NO may be functioning in clearance of OBLV60 from the CNS.

In support of the conclusion that iNOS or NO is not the sole mechanism for viral clearance are the studies of OBLV60 infection of GKO mice. These mice have been shown to lack a variety of immune functions, including the ability to produce NO (12). This is consistent with the observation that the GKO mice did not exhibit a dramatic increase in NO_2^-/NO_3^- levels in plasma compared to those of BALB/c mice following i.p. injection of LPS. The OBLV60-infected GKO mice expressed low levels of iNOS mRNA and protein in the olfactory bulb, yet did not die and were eventually able to clear virus by 18 days p.i. Similar numbers of $CD4^+$ and $CD8^+$ T lymphocytes were observed in the brains of infected GKO mice and infected BALB/c mice at 7 days p.i. (data not shown). It is possible that these cells are contributing to clearance of OBLV60 by mechanisms which are as yet unidentified.

In the mouse, IFN-γ appears to be the predominant cytokine required for high-level expression of iNOS activity. The lack of a large increase in the number of NOS-expressing cells in nude and GKO mice most likely is a reflection of the absence of IFN-γ and/or IFN-γ-producing T cells. Nude mice did exhibit a marginal increase in iNOS-positive cells at day 6 p.i., and this may be due to the presence of IFN-γ production by natural killer cells. Furthermore, Pearce et al. (36) have previously shown that OBLV60-infected nude mice expressed increased levels of mRNAs for a variety of cytokines, including TNF-α and IL-1, in the brain. It is possible that these cytokines, along with others, may induce expression of iNOS mRNA and protein in resident as well as inflammatory cells, yet the level of protein expression is so low that it is below the limit of detection. Although we have not yet determined the cytokine profile in GKO mice following infection with OBLV60, it is reasonable to suggest that inflammatory cytokines which account for the low-level expression of iNOS mRNA and protein observed in these mice are present.

The fact that the GKO mice were able to clear infectious virus is interesting and suggests that IFN-γ is not solely responsible for viral clearance in the CNS. This observation is consistent with a previous report by Smith et al. (43) which demonstrated that treatment of MHV-JHM-infected mice with recombinant IFN-γ resulted in a significant decrease in viral titers in the liver yet had no effect on viral replication in the brain. Thus, the MHV-OBLV60 model for viral clearance from the CNS appears to differ from other models showing a prominent role for IFN-γ in host defense against infection of the CNS by viruses such as measles and Theiler's viruses (15, 38). However, GKO mice suffering from an acute infection with lymphocytic choriomeningitis virus were able to clear virus, yet IFN-γ was found to have an essential role in viral clearance in persistently infected mice (46). The role of IFN-γ in mice suffering from chronic infection with MHV has yet to be determined, and IFN-γ may prove to have important contributions to either host defense or the disease process.

It is important to recognize a fundamental difference in the MHV strains we have utilized for these studies. OBLV60, used in the present studies, is a neuronotropic virus which does not normally persist in the brains of immunocompetent mice and remains primarily associated with neuronal tracts. Other strains, such as the demyelinating variant MHV-V5A13.1 (13), infect both neurons and white matter areas and cause extensive CNS demyelination. An interesting question which remains to be addressed is to what extent iNOS expression contributes to the demyelinating process in mice chronically infected with MHV. NO has previously been shown to be toxic to oligodendrocytes (30), and we have observed iNOS expression by astrocytes in demyelinating lesions in the spinal cords of mice infected 32 days earlier with MHV-V5A13.1 (23a). Sun et al. (44) have recently demonstrated that iNOS as well as the cytokines TNF-α, IL-1β, and IL-6 are expressed in the brains and spinal cords of mice chronically infected with MHV. Furthermore, Cross et al. (11) have demonstrated that administration of AG ameliorates demyelination in mice suffering from EAE, suggesting a role for iNOS and NO in demyelination. We are currently investigating the role of iNOS and NO in acute and chronic demyelinating disease following infection with MHV.

ACKNOWLEDGMENTS

We thank Iain Campbell, Howard Fox, and Lindsay Whitton for helpful advice and discussion and Jim Johnston for manuscript preparation.

This work was supported by NIH grants AI 25913 and MH 19185. T.E.L. is a postdoctoral fellow of the National Multiple Sclerosis Society.

REFERENCES

1. **Akarid, K., M. Sinet, B. Desforges, and M. Gougerot-Pocidalo.** 1995. Inhibitory effect of nitric oxide on the replication of a murine retrovirus in vitro and in vivo. J. Virol. **69:**7001–7005.
2. **Baier, M., A. Werner, N. Banner, K. Metzner, and R. Kurth.** 1995. HIV suppression by interleukin-16. Nature **378:**563.
3. **Bi, Z., M. Barna, T. Komatsu, and C. Reiss.** 1995. Vesicular stomatitis virus infection of the central nervous system activates both innate and acquired immunity. J. Virol. **69:**6466–6472.
4. **Bi, Z., and C. Reiss.** 1995. Inhibition of vesicular stomatitis virus infection by nitric oxide. J. Virol. **69:**2208–2213.
5. **Bredt, D., and S. Snyder.** 1992. Nitric oxide, a novel neuronal messenger. Neuron **8:**3–11.
6. **Buchmeier, M., H. Lewicki, P. Talbot, and R. Knobler.** 1984. Murine hepatitis virus-4 (strain JHM)-induced neurologic disease is modulated in vivo by monoclonal antibody. Virology **132:**261–270.
7. **Campbell, I., A. Samimi, and C.-S. Chiang.** 1994. Expression of the inducible nitric oxide synthase: correlation with neuropathology and clinical features in mice with lymphocytic choriomeningitis. J. Immunol. **153:**3622–3629.
8. **Cocchi, F., A. L. Pevico, A. Garzino-Demo, S. K. Arya, R. C. Gallo, and P. Lusso.** 1995. Identification of RANTES, MIP-1alpha, and MIP-1beta as the major HIV-suppressive factors produced by $CD8^+$ T cells. Science **270:**1811–1815.
9. **Corbett, J. A., R. G. Tilton, K. Chang, K. S. Hasan, Y. Ido, J. L. Wang, M. A. Sweetland, J. R. Lancaster, Jr., J. R. Williamson, and M. L. McDaniel.** 1992. Aminoguanidine inhibits nitric oxide formation and prevents diabetic vascular dysfunction. Diabetes **41:**552–556.
10. **Croen, K.** 1993. Evidence for an antiviral effect of nitric oxide. J. Clin. Invest. **91:**2446–2452.
11. **Cross, A. H., T. Misko, R. Lin, W. Hickey, J. Trotter, and R. Tilton.** 1994. Aminoguanidine, an inhibitor of inducible nitric oxide synthase, ameliorates experimental autoimmune encephalomyelitis in SJL mice. J. Clin. Invest. **93:**2684–2690.
12. **Dalton, D. K., S. Pitts-Meek, S. Keshav, I. S. Figari, A. Bradley, and T. A. Stewart.** 1993. Multiple defects of immune cell function in mice with disrupted interferon-gamma genes. Science **259:**1739–1742.
13. **Dalziel, R. G., P. W. Lampert, P. J. Talbot, and M. J. Buchmeier.** 1986. Site-specific alteration of murine hepatitis virus type 4 peplomer glycoprotein E2 results in reduced neurovirulence. J. Virol. **59:**463–471.
14. **Feduchi, E., M. A. Alonso, and L. Carrasco.** 1989. Human gamma interferon and tumor necrosis factor exert a synergistic blockade on the replication of herpes simplex virus. J. Virol. **63:**1354–1359.
15. **Finke, D., U. G. Brinckmann, V. terMeulen, and U. G. Liebert.** 1995. Gamma interferon is a major mediator of antiviral defense in experimental measles virus-induced encephalitis. J. Virol. **69:**5469–5474.
16. **Gallagher, T. M., C. Escarmis, and M. J. Buchmeier.** 1991. Alteration of the pH dependence of coronavirus-induced cell fusion: effect of mutations in the spike glycoprotein. J. Virol. **65:**1916–1928.
17. **Harris, N., M. L. Buller, and G. Karupiah.** 1995. Gamma interferon-induced, nitric oxide-mediated inhibition of vaccinia virus replication. J. Virol. **69:**910–915.
18. **Hirano, N., N. Goto, S. Makino, and K. Fujiwara.** 1978. Utility of mouse cell line DBT for propagation and assay of mouse hepatitis virus. Jpn. J. Exp. Med. **48:**71–75.
19. **Hooper, D. C., S. T. Ohnishi, R. Kean, Y. Numagami, B. Dietzschold, and H. Koprowski.** 1995. Local nitric oxide production in viral and autoimmune diseases of the central nervous system. Proc. Natl. Acad. Sci. USA **92:**5312–5316.
20. **Ignarro, L., H. Lippton, J. Edwards, W. Baricos, A. Hyman, P. Kudowitz, and C. Cruetter.** 1981. Mechanism of vascular smooth muscle relaxation by organic nitrates, nitrites, nitroprusside, and nitric oxide: evidence for the involvement of *S*-nitrosothiols as active intermediates. J. Pharmacol. Exp. Ther. **218:**739–749.
21. **Karupiah, G., Q. Xie, R. Buller, C. Nathan, C. Duarte, and J. MacMicking.** 1993. Inhibition of viral replication by interferon-gamma-induced nitric oxide synthase. Science **261:**1445–1446.
22. **Koprowski, H., Y. Zheng, E. Heber-Katz, N. Fraser, L. Rorke, F. Fangfu, C. Hanlon, and B. Dietzschold.** 1993. In vivo expression of inducible nitric oxide synthase in experimentally induced neurologic diseases. Proc. Natl. Acad. Sci. USA **90:**3024–3027.
23. **Kreil, T. R., and M. M. Eibl.** 1996. Nitric oxide and viral infection: no antiviral activity against a flavivirus in vitro, and evidence for contribution to pathogenesis in experimental infection in vivo. Virology **219:**304–306.

23a. **Lane, T. E., and M. J. Buchmeier.** Unpublished data.

24. **Levine, B., J. Hardwick, B. Trapp, T. Crawford, R. Bollinger, and D. Griffin.** 1991. Antibody-mediated clearance of alphavirus infection from neurons. Science **254:**856–860.
25. **Lin, R. F., T.-S. Lin, R. G. Tilton, and A. H. Cross.** 1993. Nitric oxide localized to spinal cords of mice with experimental allergic encephalomyelitis: an electron paramagnetic resonance study. J. Exp. Med. **178:**643–648.
26. **Lowenstein, C. J., S. L. Hill, A. Lafond-Walker, J. Wu, G. Allen, M. Landavere, N. R. Rose, and A. Herskowitz.** 1996. Nitric oxide inhibits viral replication in murine myocarditis. J. Clin. Invest. **97:**1837–1843.
27. **Lowenstein, C. J., C. S. Glatt, D. S. Bredt, and S. H. Snyder.** 1992. Cloned and expressed macrophage nitric oxide synthase contrasts with the brain enzyme. Proc. Natl. Acad. Sci. USA **89:**6711–6715.
28. **Marletta, M. A., P. S. Yoon, R. Iyengar, C. D. Leaf, and J. S. Wishnok.** 1988. Macrophage oxidation of L-arginine to nitrite and nitrate: nitric oxide is an intermediate. Biochemistry **27:**8706–8711.
29. **Melkova, Z., and M. Esteban.** 1995. Inhibition of vaccinia virus DNA replication by inducible expression of nitric oxide synthase. J. Immunol. **155:**5711–5718.
30. **Merrill, J. E., L. J. Ignarro, M. P. Sherman, J. Melinek, and T. E. Lane.** 1993. Microglial cell cytotoxicity of oligodendrocytes is mediated through nitric oxide. J. Immunol. **151:**2132–2141.
31. **Misko, T. P., W. M. Moore, T. P. Kasten, G. A. Nickols, J. A. Corbett, R. G. Tilton, M. L. McDaniel, J. R. Williamson, and M. G. Currie.** 1993. Selective inhibition of the inducible nitric oxide synthase enzyme by aminoguanidine. Eur. J. Pharmacol. **233:**119–122.
32. **Moncada, S., R. Palmer, and E. Higgs.** 1991. Nitric oxide: physiology, pathophysiology, and pharmacology. Pharmacol. Rev. **43:**109–142.
33. **Nathan, C., and J. Hibbs.** 1991. Role of nitric oxide synthesis in macrophage antimicrobial activity. Curr. Opin. Immunol. **3:**65–70.
34. **Nathan, C., and Q. Xie.** 1994. Nitric oxide synthases: roles, tolls, and controls. Cell **78:**915–918.
35. **Oldstone, M. B. A., P. Blount, P. Southern, and P. Lampert.** 1986. Cytoimmunotherapy for persistent virus infection reveals a unique clearance pattern from the central nervous system. Nature **321:**239–243.
36. **Pearce, B. D., M. V. Hobbs, T. S. McGraw, and M. J. Buchmeier.** 1994. Cytokine induction during T-cell-mediated clearance of mouse hepatitis virus from neurons in vivo. J. Virol. **68:**5483–5495.
37. **Ramsay, A., J. Ruby, and I. Ramshaw.** 1993. A case for cytokines as effector molecules in the resolution of virus infection. Immunol. Today **14:**155–157.
38. **Rodriguez, M., K. Pavelko, and R. Coffman.** 1995. Gamma interferon is critical for resistance to Theiler's virus-induced demyelination. J. Virol. **69:**7286–7290.
39. **Rolph, M. S., I. A. Ramshaw, K. A. Rockett, J. Ruby, and W. B. Cowden.** 1996. Nitric oxide production is increased during murine vaccinia virus infection, but may not be essential for virus clearance. Virology **217:**470–477.
40. **Ryder, E., E. Snyder, and C. Lepko.** 1990. Establishment and characterization of multipotent neural cell lines using retrovirus vector-mediated oncogene transfer. J. Neurobiol. **21:**356–375.
41. **Sambrook, J., E. F. Fritsch, and T. Maniatis.** 1989. Molecular cloning: a laboratory manual, 2nd ed. Cold Spring Harbor Laboratory Press, Cold Spring Harbor, N.Y.
42. **Simmons, M. L., and S. Murphy.** 1992. Induction of nitric oxide synthase in glial cells. J. Neurochem. **59:**897–905.
43. **Smith, A., S. Barthold, M. de Souza, and K. Bottomly.** 1991. The role of gamma interferon in infection of susceptible mice with murine coronavirus, MHV-JHM. Arch. Virol. **121:**89–100.
44. **Sun, N., D. Grzybicki, R. F. Castro, S. Murphy, and S. Perlman.** 1995. Activation of astrocytes in the spinal cord of mice chronically infected with a neurotropic coronavirus. Virology **213:**482–493.
45. **Sussman, M. A., R. A. Shubin, S. Kyuwa, and S. A. Stohlman.** 1989. T-cell-mediated clearance of mouse hepatitis virus strain JHM from the central nervous system. J. Virol. **63:**3051–3056.
46. **Tishon, A., H. Lewicki, G. Rall, M. von Herrath, and M. B. A. Oldstone.** 1995. An essential role for type-1 interferon-γ in terminating persistent viral infection. Virology **212:**244–250.
47. **Tucker, P. C., D. E. Griffin, S. Choi, N. Bui, and S. Wesselingh.** 1996. Inhibition of nitric oxide synthesis increases mortality in Sindbis virus encephalitis. J. Virol. **70:**3972–3977.
48. **Williamson, J. S. P., and S. A. Stohlman.** 1990. Effective clearance of mouse hepatitis virus from the central nervous system requires both $CD4^+$ and $CD8^+$ T cells. J. Virol. **64:**4589–4592.
49. **Zheng, Y. M., M. K.-H. Schafer, E. Weihe, H. Sheng, S. Corisdeo, Z. F. Fu, H. Koprowski, and B. Dietzschold.** 1993. Severity of neurological signs and degree of inflammatory lesions in the brains of rats with Borna disease correlate with the induction of nitric oxide synthase. J. Virol. **67:**5786–5791.
50. **Zinkernagel, R. M.** 1993. Immunity to viruses, p. 1211–1250. *In* W. E. Paul (ed.), Fundamental immunology, 3rd ed. Raven Press, New York, N.Y.